

Article

Improvement of RF Wireless Power Transmission Using a Circularly Polarized Retrodirective Antenna Array with EBG Structures

Son Trinh-Van, Jong Min Lee, Youngoo Yang, Kang-Yoon Lee and Keum Cheol Hwang * 

School of Electronic and Electrical Engineering, Sungkyunkwan University, Suwon 440-746, Korea; jsonbkhn@gmail.com (S.T.-V.); ljm4081@naver.com (J.M.L.); yang09@skku.edu (Y.Y.); klee@skku.edu (K.-Y.L.)

* Correspondence: khwang@skku.edu; Tel.: +82-31-290-7978

Received: 14 December 2017; Accepted: 22 February 2018; Published: 26 February 2018

Abstract: This paper presents the performance improvement of a circularly polarized (CP) retrodirective array (RDA) through the suppression of mutual coupling effects. The RDA is designed based on CP Koch-shaped patch antenna elements with an inter-element spacing as small as 0.4λ for a compact size (λ is the wavelength in free space at the designed frequency of 5.2 GHz). Electromagnetic band gap (EBG) structures are applied to reduce the mutual coupling between the antenna elements, thus improving the circular polarization characteristic of the RDA. Two CP RDAs with EBGs, in the case 5×5 and 10×10 arrays, are used as wireless power transmitters to transmit a total power of 50 W. A receiver is located at a distance of 1 m away from the transmitter to harvest the transmitted power. At the broadside direction, the simulated results demonstrate that the received powers are improved by approximately 11.32% and 12.45% when using the 5×5 and 10×10 CP RDAs with the EBGs, respectively, as the transmitters.

Keywords: circular polarization; EBG structure; Koch-shaped patch antenna; retrodirective array; wireless power transmission

1. Introduction

The retrodirective array (RDA), which has the unique ability to transmit a received signal back toward the source direction without any prior information about the source location, has been the competitive choice for possible wireless communication scenarios in which high-speed target tracking and high link gain levels are desired [1]. Applications that could benefit from the use of an RDA include solar power satellites [2,3], vehicle radars [4], and wireless power transmission systems [5].

The well-known techniques for realizing an RDA consist of a corner reflector, the Van Atta array [6], and a heterodyne RDA integrated with an RF circuit for phase conjugation [7]. Because compact and planar topologies are highly desired in modern wireless communications, most of the reported RDAs were based on Van Atta arrays and on heterodyne RDA arrays [8–12]. In these RDAs, radiating elements were designed with a linear polarization operation. Therefore, when the incident waves are also linearly polarized (LP) waves, the reflected or scattering waves retain the same polarization. Consequently, the scattering and retrodirective signals are mixed, making it difficult to extract the retrodirective signal from the total bistatic radar cross-section (BRCS) response. In order to overcome this problem, an RDA capable of polarization rotation was introduced [13]. However, with this technique, the transmitting and receiving antennas must be designed with different polarizations, thus increasing the cost and size of the overall system. Therefore, the RDA with circular polarization becomes a promising solution for use in an RDA system. In a circularly polarized (CP) RDA system, the reflected or scattering waves are orthogonal to the incident waves, while the polarization state of the retrodirective waves is identical to that of the incident waves. Consequently,

the same antenna can be used as the transmitting and receiving antennas, hence improving the compactness and reducing the cost of the overall system. However, there are very limited works on the design of RDAs with circular polarization in the literature [14–16].

In this paper, we investigate a technique to enhance the performance of a CP RDA. The CP RDA is designed using an array of CP Koch-shaped patch antennas [17]. To achieve a compact size array, the inter-element spacing is decreased to 0.4λ (λ is the wavelength in free space at the designed frequency of 5.2 GHz). Because the inter-element spacing is small, the mutual coupling effects become critical and considerably affect the CP behavior of the RDA. EBG structures are then implemented between the antenna elements to reduce the mutual coupling. The performance of the CP RDA with the EBGs is verified through wireless power transmission scenarios. As a result, when the power receiver is at the broadside direction, a received power improvement of about 12.45% is achieved using the 10×10 CP RDA with the EBGs as a transmitter compared to the use of a CP RDA without the EBGs. The paper is arranged as follows. Section 2 introduces the design of the proposed CP RDA with the EBGs and its performance improvement. The performance of the CP RDA with the EBGs during a wireless power transmission assessment is presented in Section 3. Finally, the conclusion is given in Section 4.

2. Design of the Proposed RDA with the EBGs

Figure 1a demonstrates a wireless power transmission scenario of the type used in a typical indoor environment, such as an office or a living room. Inside the room, there are electronic devices, such as laptops and mobile devices, which serve as power receivers. They are located randomly at the different positions of the users and are assumed to be able to move freely. These electronic devices can be charged wirelessly from the transmitter by broadcasting pilot signals. In response to the pilot signals, the transmitter transmits power wirelessly back in the reverse direction to the electronic devices. The wireless power transmitter is a RDA which can be mounted on the ceiling or walls. In this work, the RDA is a CP microstrip patch antenna array incorporated with EBG structures, as illustrated in Figure 1b. The microstrip patch antenna is designed using the Koch fractal shape for circular polarization operation and to reduce the size. The mushroom-like EBGs are used to suppress the mutual coupling effects between antenna elements, therefore enhancing the performance of the proposed CP RDA.

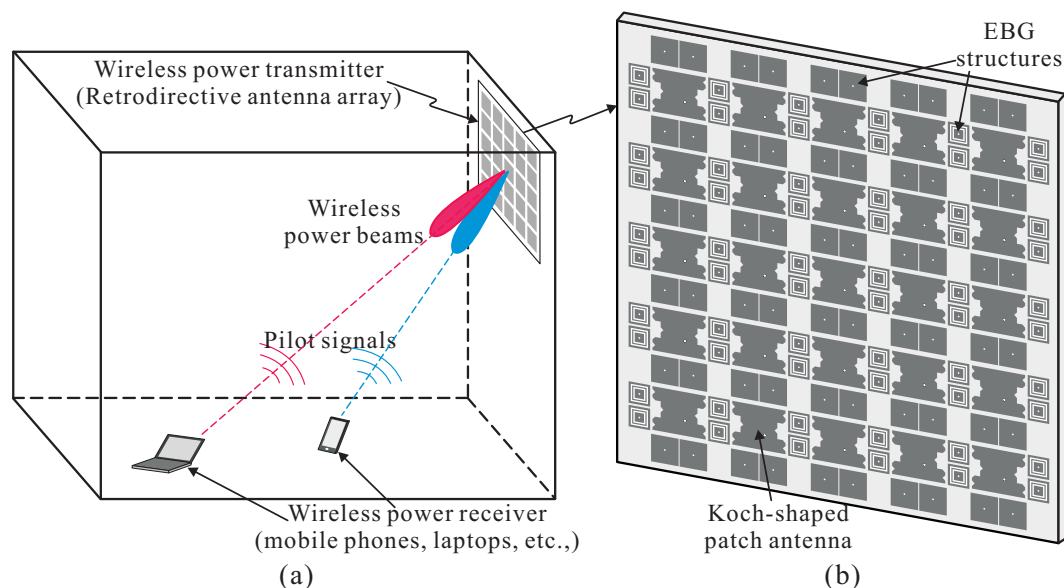


Figure 1. (a) Depiction of the wireless power transmission scheme in a typical indoor environment; (b) Configuration of the proposed CP RDA. CP RDA: Circularly polarized retrodirective array.

2.1. Mutual Coupling Reduction with the Presence of the EBGs

Figure 2a illustrates the configuration of a single CP Koch-shaped patch antenna surrounded with EBGs. The Koch fractal shape is applied into two edges along the x -direction of a rectangular patch. This Koch-shaped patch is excited through a feeding point located at distances of d_x and d_y from the center of the patch towards the $+x$ - and $-y$ -axes, respectively, to realize good circular polarization. The antenna is designed and optimized to operate at a frequency of 5.2 GHz using a previously published design process [17–20]. Both the patch and the EBGs are printed on the upper layer of a single Taconic dielectric substrate with a dielectric constant of 3.5, a thickness of 1.52 mm, and a loss tangent of 0.0019. Owing to the difference in the geometry of the Koch-shaped patch along x - and y -axes, two types of EBGs are used. A conventional mushroom-like EBG structure is located along the y -axis [21]. Meanwhile, a slot-loaded mushroom-like EBG structure, which has compact size to avoid overlapping of the patch, is placed along the x -axis [22]. By etching two rectangular slots on the metallic patch of the EBG cell, the series equivalent capacitance can be enlarged, resulting in a more compact EBG structure. Both of these EBGs are designed to suppress the mutual coupling at a frequency of 5.2 GHz. The proposed design is simulated and optimized using CST Microwave Studio software with conductor and dielectric losses taken into consideration.

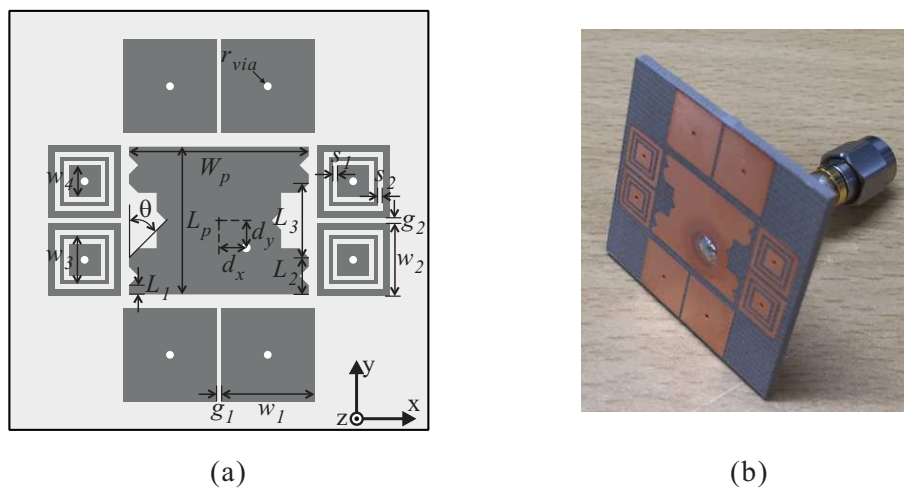


Figure 2. (a) Single CP Koch-shaped patch antenna with EBGs; (b) Photograph of the fabricated prototype. $W_p = 15.45$ mm, $L_p = 12.69$ mm, $d_x = 1.695$ mm, $d_y = 1.966$ mm, $L_1 = 0.793$ mm, $L_2 = 3.173$ mm, $L_3 = 9.516$ mm, $\theta = 45^\circ$, $w_1 = 8.0$ mm, $g_1 = 0.4$ mm, $w_2 = 6.25$ mm, $g_2 = 0.5$ mm, $w_3 = 4.2$ mm, $w_4 = 2.7$ mm, $s_1 = 0.4$ mm, $s_2 = 0.4$ mm and $r_{via} = 0.25$ mm.

The EBGs were optimized by placing one cell in the computation domain. Two perfect electric conductor (PEC) walls and two perfect magnetic conductor (PMC) walls were used to simulate the infinite-sized periodical structure [23], as shown in Figure 3a. We calculated the reflection phases of the EBGs. Simulated reflection phases are presented in Figure 3b for both the optimized conventional and slot-loaded mushroom-like EBGs with the optimized parameters listed in the caption of Figure 2. As observed in Figure 3b, the resonance frequencies for the 0° reflection phases are approximately 5.2 GHz.

A prototype of the antenna with the EBGs is fabricated using the optimized parameters, as shown in the caption; a corresponding photograph is shown in Figure 2b. The measured and simulated results of the single CP Koch-shaped patch antenna with the EBGs are depicted in Figure 4. Note that the measured results are in good agreement with the simulated results. A -10 dB reflection bandwidth of 5.12–5.30 GHz was found during the measurement. The measured axial ratio (AR) value was 2.42 at the designed frequency of 5.2 GHz; meanwhile, a minimum AR value of 1.32 dB was obtained at 5.175 GHz. The measured 3 dB AR bandwidth was 5.16–5.21 GHz. An antenna without EBGs was also

investigated, and these simulated results are included in Figure 4a,b. It can be seen that the 3 dB AR bandwidth of the proposed antenna with the EBGs was shifted slightly to a lower frequency range. Moreover, the minimum simulated AR value was reduced from 1.90 to 0.96 dB when using the EBGs, hence improving the CP purity. The radiation patterns at the designed frequency of 5.2 GHz on the two major cutting planes (the xz - and yz -planes) are shown in Figure 4c. It was found that the radiation patterns exhibit left-handed circular polarization (LHCP), in which the LHCP gain is approximately 17.1 dB higher than the right-handed circular polarization (RHCP) gain in the $+z$ -direction.

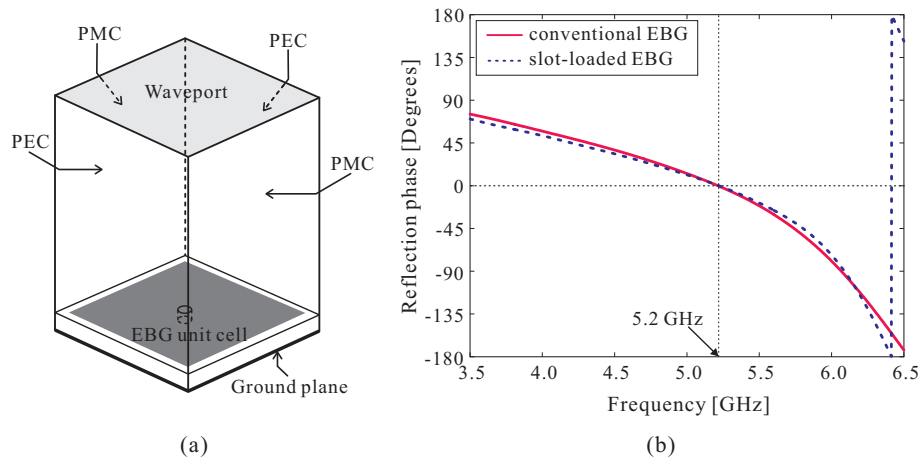


Figure 3. (a) A simulation model of an EBG structure for the calculation of the reflection phase; (b) Simulated reflection phases of EBGs. EBG: Electromagnetic band gap.

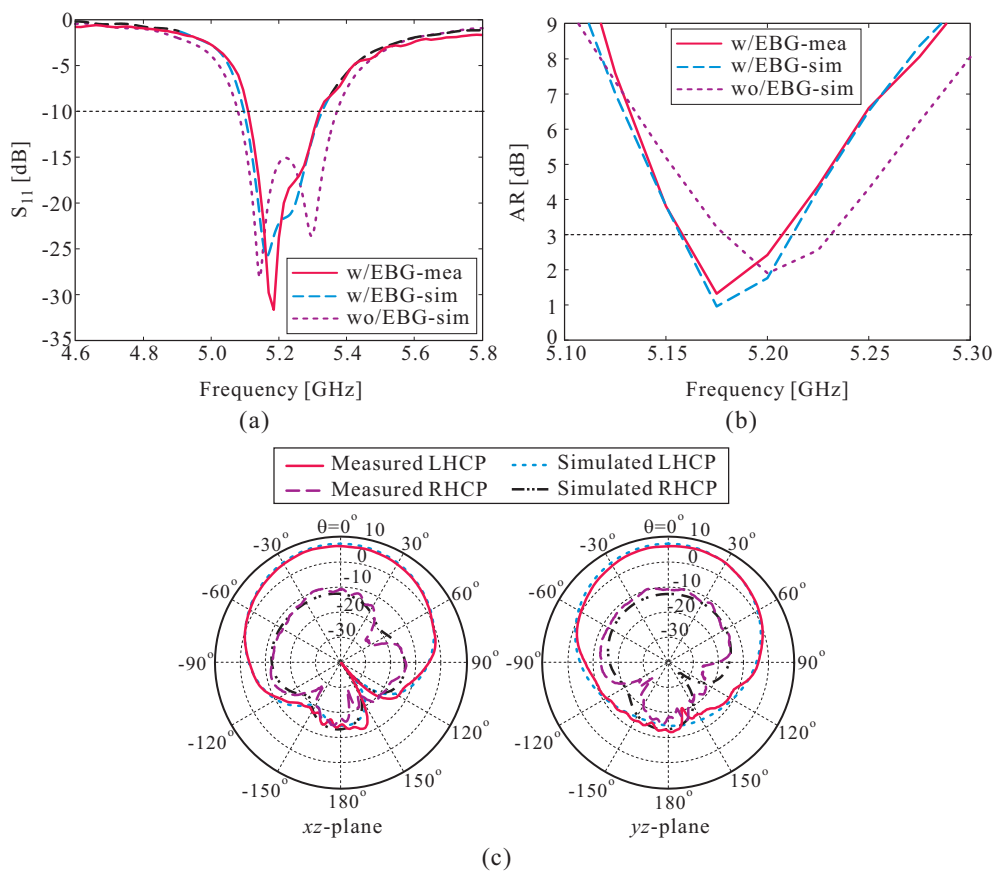


Figure 4. Measured and simulated results of the single CP Koch-shaped patch antenna with the EBGs: (a) reflection coefficients; (b) ARs; and (c) radiation patterns at 5.2 GHz. AR: Axial ratio.

To examine the performance of the EBGs for the mutual coupling reduction, a 2×2 array configuration is studied. A prototype was fabricated and a photograph was taken, as shown in Figure 5a. The antenna elements are spaced at a distance of $d = 0.4\lambda$ along the x - and y -axes (λ is the wavelength in free space at 5.2 GHz). Figure 5b plots the measured and simulated reflection coefficients of the 2×2 arrays with and without the EBGs when element #1 is excited. It can be observed that the -10 dB reflection bandwidths are centered at 5.2 GHz. The mutual coupling effects on three typical cutting planes, i.e., the horizontal, diagonal, and vertical planes, are investigated, as represented by the terms S_{21} , S_{31} and S_{41} , respectively. The results of a comparison of the measured and simulated results of S_{21} , S_{31} and S_{41} are illustrated in Figure 6. Within the operating frequency band, maximum mutual coupling reductions of 9.47 dB, 12.78 dB and 1.38 dB were obtained by measurements on the horizontal, diagonal, and vertical planes, as shown in Figure 6a–c, respectively. Meanwhile, in the simulated results, the corresponding values were 10.78 dB, 17.1 dB and 6.62 dB. Note that due to the limited spacing between two patches, only one row of EBG cells was implemented. Therefore, the bandwidth for mutual coupling reduction was very narrow, but the designed frequency of 5.2 GHz was within this bandwidth. Reasonable agreement was also achieved between the measurement and simulation. The discrepancy between the measurement and simulation results was mainly attributed to experimental tolerances and fabrication imperfections, especially the losses at the soldered joints between the coaxial cables and the patches.

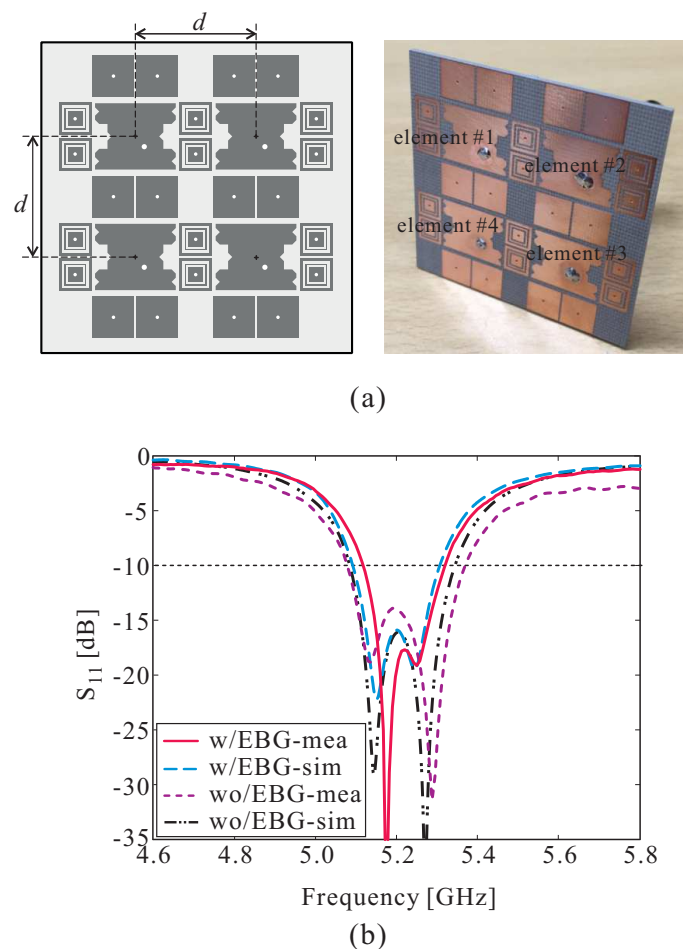
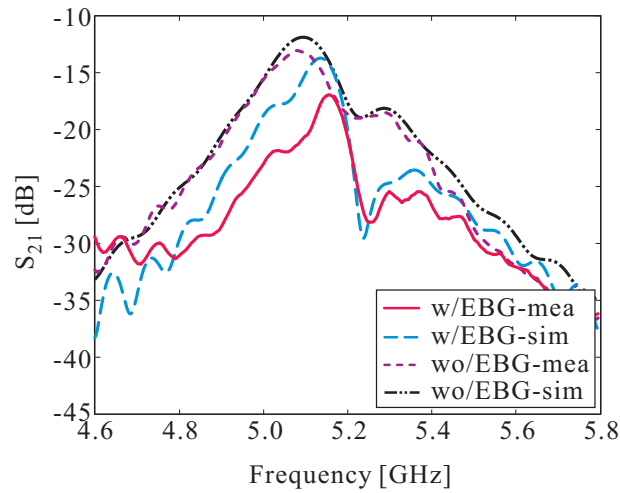
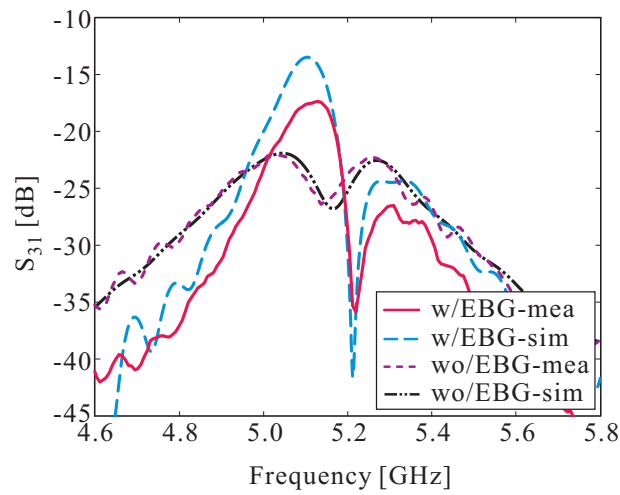


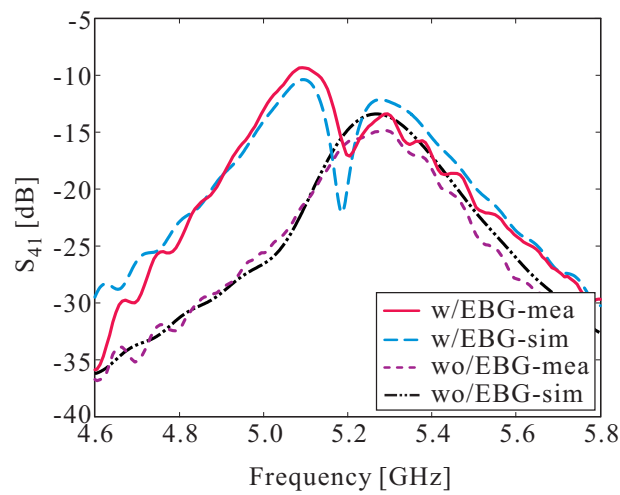
Figure 5. (a) The 2×2 array configuration for consideration of the mutual coupling and a photograph of the fabricated prototype; (b) Measured and simulated reflection coefficients of the 2×2 array with and without the EBGs.



(a)



(b)



(c)

Figure 6. Measured and simulated results of (a) S_{21} ; (b) S_{31} ; and (c) S_{41} .

2.2. Performance of RDA with the EBGs

In this section, the 5×5 array of Koch-shaped patch antenna with the EBGs is studied. The inter-element spacing is reduced to as small as 0.4λ to realize a compact size. Figure 7a shows the configuration of the 5×5 Koch-shaped patch antenna array with the EBGs. For the simulation, a port was used for each antenna element, and all ports were simultaneously excited. Performance outcomes with regard to the active reflection coefficient and the AR of the center element were investigated and presented. A comparison of the reflection coefficients and ARs for the center element of the array with and without the EBGs was conducted, with the results illustrated in Figure 7b. Note that the AR values are observed in the $+z$ -direction. It is evident that the CP performance of the array without the EBGs was considerably deteriorated due to the strong mutual coupling effects. The minimum AR value was increased to 3.83 dB. In contrast, with the EBGs, the CP performance was significantly improved. Owing to the reduced mutual coupling, the minimum AR value was reduced to 0.31 dB. At the designed frequency of 5.2 GHz, an AR value of 1.20 dB was achieved. In addition, the -10 dB reflection bandwidth was enhanced with the presence of the EBGs. The radiation patterns, when all ports were simultaneously excited, at 5.2 GHz are depicted in Figure 8 for the two major cutting planes of the xz - and yz -planes. With the EBGs to reduce mutual coupling, an approximate gain enhancement of 0.4–0.8 dB was obtained as compared to the array without the EBGs when the radiation pattern is scanned from the broadside to 60° on each plane. Therefore, the simulated results demonstrated that the presence of the EBGs significantly enhances the CP performance of the RDA despite the fact that the inter-element spacing is reduced to as small as 0.4λ .

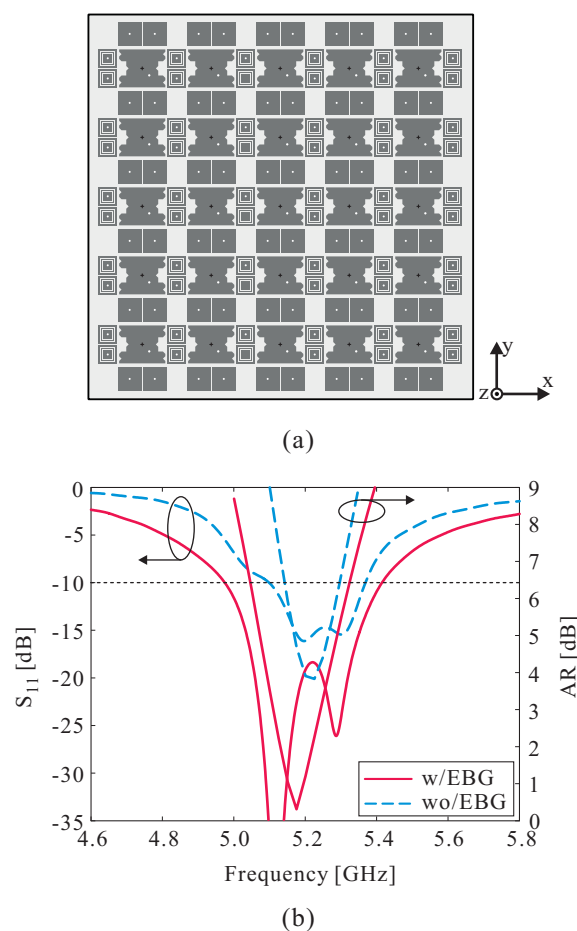


Figure 7. (a) 5×5 CP Koch-shaped patch array with the EBGs; (b) Simulated results of the reflection coefficients and ARs.

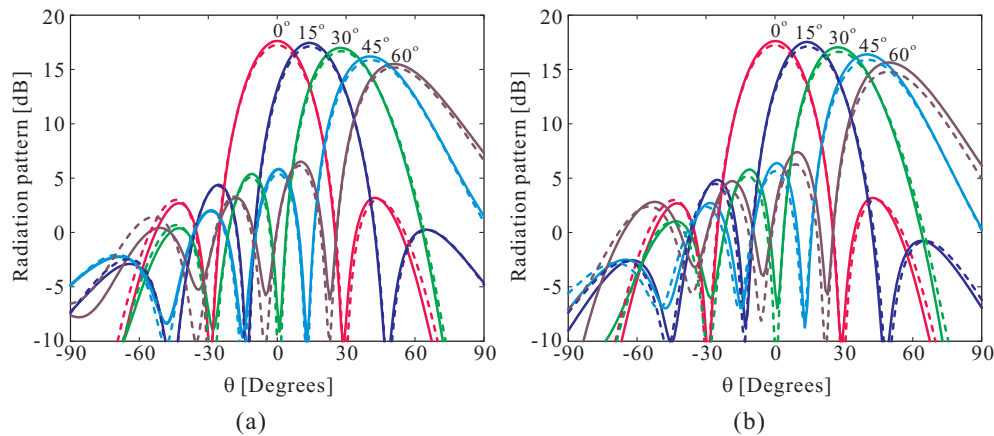


Figure 8. Simulated radiation patterns of the 5×5 CP RDA arrays with EBGs (solid line curve) and without EBGs (dashed line curve) at 5.2 GHz: (a) xz -plane and (b) yz -plane.

3. Performance in Wireless Power Transmission

The wireless power transmission performance capabilities of the proposed RDA with the EBGs are investigated. The simulation model, as shown in Figure 9, was performed using CST Microwave Studio. The receiver antenna is a single CP Koch-shaped patch antenna operating at 5.2 GHz and is located along the $+z$ -direction. Here, 5×5 Koch-shaped patch arrays with and without EBGs are used as wireless power transmitters, transmitting a total power of 50 W. The power transmitter and receiver are enclosed by a concrete box filled with air to approximate a practical indoor environment. The concrete box has overall dimensions of $2 \times 1.2 \times 1.2 \text{ m}^3$. Approximately 400 million mesh cells are used for each simulation of the wireless power transmission. All simulations are run on a computer with an Intel Core i7-5960X 3.0 GHz CPU and 128 GB of RAM integrated with two NVIDIA Quadro P6000 GPUs. The average runtime is approximately four hours for each simulation. The wireless power transmission procedure involves two steps. In the first step, only the receiver antenna was excited, and the transmission coefficient phase from the receiver antenna to each of the antenna elements of the power transmitter were recorded. The phase profile was then analyzed through phase conjugation at each antenna element. In the second step, all of the antenna elements of the power transmitter were simultaneously excited with the conjugate-phase profile, forming a wireless power beam back in the reverse direction to the power receiver. The wireless power transmission performance is evaluated by analyzing the amount of received power at the receiver. To realize a far-field retrodirective scenario, the distance between the power transmitter and the power receiver is set to 1 m. Received power of 0.2685 W was harvested by the receiver when the power was transmitted by the RDA with the EBGs. Meanwhile, when the power was transmitted by the RDA without the EBGs, only 0.2412 W of power was received. Therefore, an improvement of 11.32% is achieved using the RDA with the EBGs.

For a further investigation, three 10×10 arrays, in this case two RDAs without the EBGs having an inter-element spacing of 0.5λ and 0.4λ and one RDA with the EBGs having an inter-element spacing of 0.4λ , are used as the wireless power transmitters. The total transmitted power is 50 W. The distance between the transmitter and receiver is kept at 1 m so that a near-field retrodirective scenario is realized. The simulated results of the received powers are summarized in Table 1. For the case without EBGs, 1.339 W of power was received when using the RDA with an inter-element spacing of 0.5λ , whereas when the inter-element spacing is reduced to 0.4λ , the received power was only 0.827 W, representing a significant decrease. This reduction in the received power was mainly caused by the reduced gain which resulted when the inter-element spacing was decreased from 0.5 to 0.4λ . However, with an inter-element spacing as small as 0.4λ , the gain enhancement can be achieved by suppressing the mutual coupling effects, hence improving the received power. By using the EBGs to reduce mutual

coupling, 0.930 W of power could be harvested, showing an improvement of 12.45% compared to the CP RDA without the EBGs.

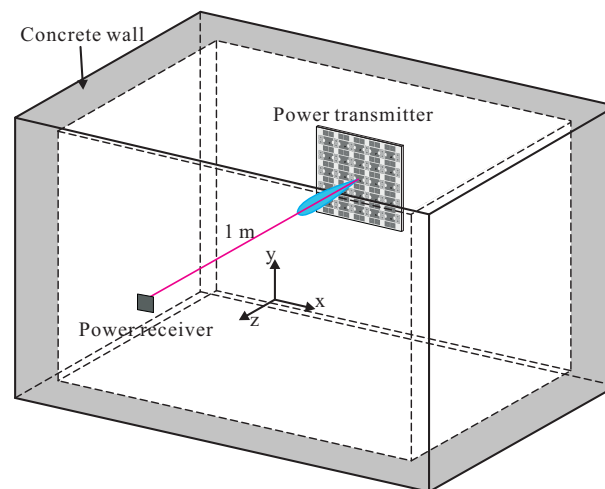


Figure 9. Simulation model for wireless power transmission.

Finally, the wireless power transmission performance capabilities when the power receiver moves along the x - and y -directions were investigated. Here, 10×10 CP RDA arrays with and without EBGs and with an inter-element spacing of 0.4λ are used as transmitters to transmit a total power of 50 W. The simulated electric field distribution at 5.2 GHz, when the power receiver is located off the broadside direction, is illustrated in Figure 10. It can be observed that the electromagnetic wave propagates in a direction toward the location of the power receiver. Table 2 summarizes the simulated results of the received power outputs, as harvested by the power receiver as a result of the power transmitted by the 10×10 CP RDA arrays with and without the EBGs. Clearly, the amount of received power was reduced as the power receiver was moved away from the broadside direction. However, as demonstrated in Table 2, the use of the EBGs resulted in a significant improvement in the received power due to the reduced mutual coupling. An improvement which ranged from 12.91 to 21.02% was obtained as compared to the case without EBGs when the power receiver moves along the x - and y -directions. This again validates the performance enhancement of the proposed CP RDA with EBGs during wireless power transmission.

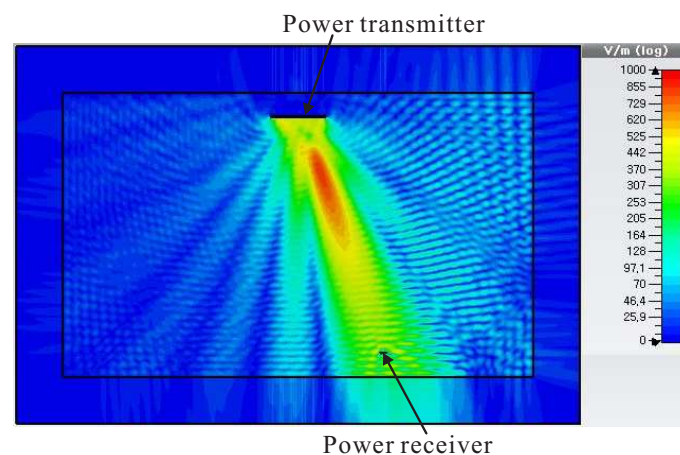


Figure 10. Simulated electric field distribution at 5.2 GHz when moving the power receiver away from the broadside direction.

Table 1. Comparison of the received power when using the 10×10 CP RDAs with and without the EBGs (where λ is free space wavelength at the designed frequency of 5.2 GHz).

	Without EBGs		With EBGs
Inter-element Spacing	0.5λ	0.4λ	0.4λ
Received Power (W)	1.339	0.827	0.930

Table 2. Comparison of the received power when moving the power receiver along the x - and y -directions.

		Received Power (W)	Improvement (%)
Moving along x -direction	0.18 m	With EBGs	0.881
		Without EBGs	0.728
	0.36 m	With EBGs	0.649
		Without EBGs	0.539
Moving along y -direction	0.18 m	With EBGs	0.879
		Without EBGs	0.754
	0.36 m	With EBGs	0.656
		Without EBGs	0.581

4. Conclusions

In this paper, a technique to improve the performance of a CP RDA was investigated. The CP RDA consists of an array of CP Koch-shaped patch antennas with an inter-element spacing of 0.4λ for a compact size. To reduce the mutual coupling effects between antenna elements, EBG structures are applied. The performance of the CP RDA with the EBGs is validated through a wireless power transmission scenario. Owing to the mutual coupling reduction, at the broadside direction, improvements of approximately 11.32% and 12.45% were realized using 5×5 and 10×10 CP RDAs with EBGs, respectively, as wireless power transmitters in comparison to the use of RDAs without the EBGs. Improvements of 12.91–21.02% were also achieved when the power receiver was moved away from the broadside direction. This validates the performance enhancement of the proposed CP RDA incorporating the EBGs. Future work will involve the fabrication of the proposed CP RDA with EBG structures and its implementation in a wireless power transmission system for experimental verification.

Acknowledgments: This work was supported by the National Research Foundation of Korea (NRF) grant funded by the Korean government (MSIP) (2014R1A5A1011478).

Author Contributions: The presented work was carried out in collaboration of all authors. Son Trinh-Van and Jong Min Lee performed the simulations. Youngoo Yang, Kang-Yoon Lee, and Keum Cheol Hwang participated to the conception, fabrication and experiment. Son Trinh-Van wrote the paper which was edited by all co-authors.

Conflicts of Interest: The authors declare no conflict of interest.

References

- Goshi, D.S.; Leong, K.M.K.H.; Itoh, T. Recent advances in retrodirective system technology. In Proceedings of the 2006 IEEE Radio and Wireless Symposium, San Diego, CA, USA, 17–19 October 2006; pp. 459–462.
- Matsumoto, H. Research on solar power satellites and microwave power transmission in Japan. *IEEE Microw. Mag.* **2002**, *3*, 36–45.
- Mekikis, P.V.; Kartsakli, E.; Antonopoulos, A.; Alonso, L.; Verikoukis, C. Connectivity analysis in clustered wireless sensor networks powered by solar energy. *IEEE Trans. Wirel. Commun.* **2018**, *PP*, 1.

4. Fusco, V.F. Retrodirective array techniques for ACC vehicular augmentation. In Proceedings of the IEE Colloquium on Antennas for Automotives (Ref. No. 2000/002), London, UK, 10 March 2000.
5. Li, Y.; Jandhyala, V. Design of retrodirective antenna array for short-range wireless power transmission. *IEEE Trans. Antennas Propag.* **2012**, *60*, 206–211.
6. Sharp, E.D.; Diab, M.A. Van Atta reflector array. *IRE Trans. Antennas Propag.* **1960**, *8*, 436–438.
7. Pon, C.Y. Retrodirective array using the heterodyne technique. *IEEE Trans. Antennas Propag.* **1964**, *12*, 176–180.
8. Ali, A.A.M.; El-Shaarawy, H.B.; Aubert, H. Millimeter-wave substrate integrated waveguide passive Van Atta reflector array. *IEEE Trans. Antennas Propag.* **2013**, *61*, 1465–1470.
9. Tseng, W.-J.; Chung, S.-B.; Chang, K. A planar Van Atta array reflector with retrodirectivity in both E-plane and H-plane. *IEEE Trans. Antennas Propag.* **2000**, *48*, 173–175.
10. Fusco, V.F.; Buchanan, N. Retrodirective array performance in the presence of near field obstructions. *IEEE Trans. Antennas Propag.* **2010**, *58*, 982–986.
11. Wang, X.; Lu, M. Microwave power transmission based on retro-reflective beamforming. In *Wireless Power Transfer—Fundamentals and Technologies*; Coca, E., Ed.; In Tech: London, UK, 2016.
12. Wang, X.; Sha, S.; He, J.; Guo, L.; Lu, M. Wireless power delivery to low-power mobile devices based on retro-reflective beamforming. *IEEE Antennas Wirel. Propag. Lett.* **2014**, *13*, 919–922.
13. Zhou, H.; Hong, W.; Tian, L.; Jiang, X.; Zhu, X.-C.; Jiang, M.; Cheng, L.; Zhuang, J.-X. A retrodirective antenna array with polarization rotation property. *IEEE Trans. Antennas Propag.* **2014**, *62*, 4081–4088.
14. Ren, Y.-J.; Chang, K. New 5.8-GHz circularly polarized retrodirective rectenna arrays for wireless power transmission. *IEEE Trans. Microw. Theory Tech.* **2006**, *54*, 2970–2976.
15. Miao, Z.-W.; Hao, Z.-C.; Yuan, Q. A passive circularly polarized Van Atta reflector for vehicle radar applications. *IEEE Antennas Wirel. Propag. Lett.* **2017**, *16*, 2254–2257.
16. Fairouz, M.; Saed, M. A retrodirective array with reduced surface waves for wireless power transfer applications. *Prog. Electromagn. Res. C* **2014**, *55*, 179–186.
17. Zhang, X.; Cheng, Z.; Gui, Y. Design of a new built-in UHF multi-frequency antenna sensor for partial discharge detection in high-voltage switchgears. *Sensors* **2016**, *16*, 1170.
18. Fukusako, T. Broadband characterization of circularly polarized waveguide antennas using L-shaped probe. *J. Electromagn. Eng. Sci.* **2017**, *17*, 1–8.
19. Jin, Y.; Tak, J.; Choi, J. Quadruple band-notched trapezoid UWB antenna with reduced gains in notch bands. *J. Electromagn. Eng. Sci.* **2016**, *16*, 35–43.
20. Ha-Van, N.; Seo, C. A single-feed port HF-UHF dual-band RFID tag antenna. *J. Electromagn. Eng. Sci.* **2017**, *17*, 233–237.
21. Yang, F.; Rahmat-Samii, Y. *Electromagnetic Band Gap Structures in Antenna Engineering*; Cambridge University Press: Cambridge, UK, 2009.
22. Azarbar, A.; Ghalibafan, J. A compact low-permittivity dual-layer EBG structure for mutual coupling reduction. *Int. J. Antennas Propag.* **2011**, *2011*, 237454.
23. Lamminen, A.E.I.; Vimpari, A.R.; Saily, J. UC-EBG on LTCC for 60-GHz frequency band antenna applications. *IEEE Trans. Antennas Propag.* **2009**, *57*, 2904–2912.

